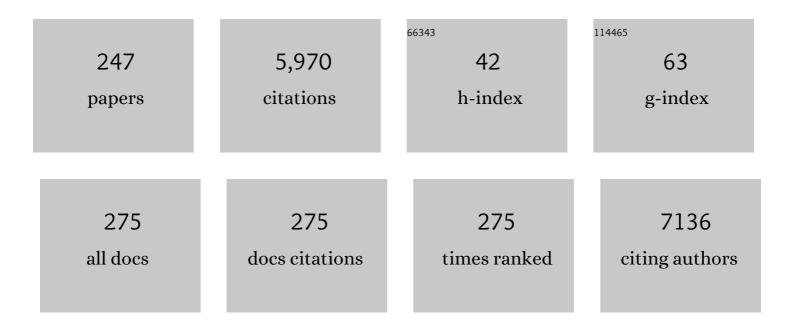
Markus Mitterhauser

List of Publications by Year in descending order

Source: https://exaly.com/author-pdf/8700130/publications.pdf Version: 2024-02-01



#	Article	IF	CITATIONS
1	Reduced Serotonin-1A Receptor Binding in Social Anxiety Disorder. Biological Psychiatry, 2007, 61, 1081-1089.	1.3	276
2	Normative database of the serotonergic system in healthy subjects using multi-tracer PET. NeuroImage, 2012, 63, 447-459.	4.2	126
3	Prediction of SSRI treatment response in major depression based on serotonin transporter interplay between median raphe nucleus and projection areas. NeuroImage, 2012, 63, 874-881.	4.2	124
4	Synthesis of fluorine-18-labeled ciprofloxacin for PET studies in humans. Nuclear Medicine and Biology, 2003, 30, 285-291.	0.6	123
5	11C-Acetate Positron Emission Tomography Imaging and Image Fusion With Computed Tomography and Magnetic Resonance Imaging in Patients With Recurrent Prostate Cancer. Journal of Clinical Oncology, 2006, 24, 2513-2519.	1.6	114
6	PSMA Ligand PET/MRI for Primary Prostate Cancer: Staging Performance and Clinical Impact. Clinical Cancer Research, 2018, 24, 6300-6307.	7.0	112
7	Differential modulation of the default mode network via serotonin-1A receptors. Proceedings of the National Academy of Sciences of the United States of America, 2012, 109, 2619-2624.	7.1	109
8	Pgp-Mediated Interaction Between (R)-[11C]Verapamil and Tariquidar at the Human Blood–Brain Barrier: A Comparison With Rat Data. Clinical Pharmacology and Therapeutics, 2012, 91, 227-233.	4.7	108
9	EANM guideline for radionuclide therapy with radium-223 of metastatic castration-resistant prostate cancer. European Journal of Nuclear Medicine and Molecular Imaging, 2018, 45, 824-845.	6.4	108
10	Basics and principles of radiopharmaceuticals for PET/CT. European Journal of Radiology, 2010, 73, 461-469.	2.6	104
11	Response assessment using 68Ga-PSMA ligand PET in patients undergoing 177Lu-PSMA radioligand therapy for metastatic castration-resistant prostate cancer. European Journal of Nuclear Medicine and Molecular Imaging, 2019, 46, 1063-1072.	6.4	100
12	Global decrease of serotonin-1A receptor binding after electroconvulsive therapy in major depression measured by PET. Molecular Psychiatry, 2013, 18, 93-100.	7.9	98
13	Sorafenib attenuates the portal hypertensive syndrome in partial portal vein ligated rats. Journal of Hepatology, 2009, 51, 865-873.	3.7	95
14	Glioma Survival Prediction with Combined Analysis of In Vivo ¹¹ C-MET PET Features, Ex Vivo Features, and Patient Features by Supervised Machine Learning. Journal of Nuclear Medicine, 2018, 59, 892-899.	5.0	94
15	Positron emission tomography imaging of adrenal masses: 18F-fluorodeoxyglucose and the 11?-hydroxylase tracer 11C-metomidate. European Journal of Nuclear Medicine and Molecular Imaging, 2004, 31, 1224-30.	6.4	93
16	Influence of escitalopram treatment on 5-HT1A receptor binding in limbic regions in patients with anxiety disorders. Molecular Psychiatry, 2009, 14, 1040-1050.	7.9	87
17	Spatial analysis and high resolution mapping of the human whole-brain transcriptome for integrative analysis in neuroimaging. NeuroImage, 2018, 176, 259-267.	4.2	87
18	Aggression is related to frontal serotoninâ€1A receptor distribution as revealed by PET in healthy subjects. Human Brain Mapping, 2009, 30, 2558-2570.	3.6	84

#	Article	IF	CITATIONS
19	In vitro and in vivo evaluation of [18F]ciprofloxacin for the imaging of bacterial infections with PET. European Journal of Nuclear Medicine and Molecular Imaging, 2005, 32, 143-150.	6.4	77
20	High-Dose Testosterone Treatment Increases Serotonin Transporter Binding in Transgender People. Biological Psychiatry, 2015, 78, 525-533.	1.3	75
21	Uptake of bone-seekers is solely associated with mineralisation! A study with 99mTc-MDP, 153Sm-EDTMP and 18F-fluoride on osteoblasts. European Journal of Nuclear Medicine and Molecular Imaging, 2006, 33, 491-494.	6.4	74
22	Lateralization of the serotonin-1A receptor distribution in language areas revealed by PET. NeuroImage, 2009, 45, 598-605.	4.2	72
23	Supervised machine learning enables non-invasive lesion characterization in primary prostate cancer with [68Ca]Ca-PSMA-11 PET/MRI. European Journal of Nuclear Medicine and Molecular Imaging, 2021, 48, 1795-1805.	6.4	72
24	Quantification of Task-Specific Glucose Metabolism with Constant Infusion of ¹⁸ F-FDG. Journal of Nuclear Medicine, 2016, 57, 1933-1940.	5.0	64
25	Application of image-derived and venous input functions in major depression using [carbonyl-11C]WAY-100635. Nuclear Medicine and Biology, 2013, 40, 371-377.	0.6	62
26	Log P , a yesterday's value?. Nuclear Medicine and Biology, 2017, 50, 1-10.	0.6	62
27	[68Ga]Pentixafor-PET/MRI for the detection of Chemokine receptor 4 expression in atherosclerotic plaques. European Journal of Nuclear Medicine and Molecular Imaging, 2018, 45, 558-566.	6.4	60
28	The serotonin-1A receptor distribution in healthy men and women measured by PET and [carbonyl-11C]WAY-100635. European Journal of Nuclear Medicine and Molecular Imaging, 2008, 35, 2159-2168.	6.4	59
29	Reduced task durations in functional PET imaging with [18F]FDG approaching that of functional MRI. NeuroImage, 2018, 181, 323-330.	4.2	59
30	Light-dependent alteration of serotonin-1A receptor binding in cortical and subcortical limbic regions in the human brain. World Journal of Biological Psychiatry, 2012, 13, 413-422.	2.6	57
31	[18 F]Ciprofloxacin, a New Positron Emission Tomography Tracer for Noninvasive Assessment of the Tissue Distribution and Pharmacokinetics of Ciprofloxacin in Humans. Antimicrobial Agents and Chemotherapy, 2004, 48, 3850-3857.	3.2	54
32	Cortisol plasma levels in social anxiety disorder patients correlate with serotonin-1A receptor binding in limbic brain regions. International Journal of Neuropsychopharmacology, 2010, 13, 1129-1143.	2.1	54
33	Regional differences in SERT occupancy after acute and prolonged SSRI intake investigated by brain PET. NeuroImage, 2014, 88, 252-262.	4.2	54
34	Escitalopram Enhances the Association of Serotonin-1A Autoreceptors to Heteroreceptors in Anxiety Disorders. Journal of Neuroscience, 2010, 30, 14482-14489.	3.6	52
35	Attenuated serotonin transporter association between dorsal raphe and ventral striatum in major depression. Human Brain Mapping, 2014, 35, 3857-3866.	3.6	50
36	Effects of Selective Serotonin Reuptake Inhibitors on Interregional Relation of Serotonin Transporter Availability in Major Depression. Frontiers in Human Neuroscience, 2017, 11, 48.	2.0	50

#	Article	IF	CITATIONS
37	Effects of Silexan on the Serotonin-1A Receptor and Microstructure of the Human Brain: A Randomized, Placebo-Controlled, Double-Blind, Cross-Over Study with Molecular and Structural Neuroimaging. International Journal of Neuropsychopharmacology, 2015, 18, pyu063-pyu063.	2.1	49
38	Response assessment using [⁶⁸ Ga]Gaâ€PSMA ligand PET in patients undergoing systemic therapy for metastatic castrationâ€resistant prostate cancer. Prostate, 2020, 80, 74-82.	2.3	49
39	Clinical outcome of standardized 177Lu-PSMA-617 therapy in metastatic prostate cancer patients receiving 7400 MBq every 4 weeks. European Journal of Nuclear Medicine and Molecular Imaging, 2020, 47, 713-720.	6.4	46
40	Interaction of ¹¹ C-Tariquidar and ¹¹ C-Elacridar with P-Glycoprotein and Breast Cancer Resistance Protein at the Human Blood–Brain Barrier. Journal of Nuclear Medicine, 2013, 54, 1181-1187.	5.0	45
41	Multiparametric [18F]Fluorodeoxyglucose/ [18F]Fluoromisonidazole Positron Emission Tomography/ Magnetic Resonance Imaging of Locally Advanced Cervical Cancer for the Non-Invasive Detection of Tumor Heterogeneity: A Pilot Study. PLoS ONE, 2016, 11, e0155333.	2.5	45
42	Immune Checkpoint Inhibitor Therapy Induces Inflammatory Activity in Large Arteries. Circulation, 2020, 142, 2396-2398.	1.6	45
43	The Norepinephrine Transporter in Attention-Deficit/Hyperactivity Disorder Investigated With Positron Emission Tomography. JAMA Psychiatry, 2014, 71, 1340.	11.0	44
44	Biological evaluation of 2′-[18F]fluoroflumazenil ([18F]FFMZ), a potential GABA receptor ligand for PET. Nuclear Medicine and Biology, 2004, 31, 291-295.	0.6	43
45	Prospective non-invasive evaluation of CXCR4 expression for the diagnosis of MALT lymphoma using [⁶⁸ Ga]Ga-Pentixafor-PET/MRI. Theranostics, 2019, 9, 3653-3658.	10.0	42
46	Gadoxetate-enhanced versus diffusion-weighted MRI for fused Ga-68-DOTANOC PET/MRI in patients with neuroendocrine tumours of the upper abdomen. European Radiology, 2013, 23, 1978-1985.	4.5	41
47	Association Between Osteogenesis and Inflammation During the Progression of Calcified Plaque Evaluated by ¹⁸ F-Fluoride and ¹⁸ F-FDG. Journal of Nuclear Medicine, 2017, 58, 968-974.	5.0	40
48	Pioglitazone decreases portosystemic shunting by modulating inflammation and angiogenesis in cirrhotic and non-cirrhotic portal hypertensive rats. Journal of Hepatology, 2014, 60, 1135-1142.	3.7	39
49	Machine learning classification of ADHD and HC by multimodal serotonergic data. Translational Psychiatry, 2020, 10, 104.	4.8	39
50	New aspects on the preparation of [11C]Methionine—a simple and fast online approach without preparative HPLC. Applied Radiation and Isotopes, 2005, 62, 441-445.	1.5	38
51	Pre vivo, ex vivo and in vivo evaluations of [68Ga]-EDTMP. Nuclear Medicine and Biology, 2007, 34, 391-397.	0.6	37
52	Central serotonin 1A receptor binding in temporal lobe epilepsy: A [carbonyl-11C]WAY-100635 PET study. Epilepsy and Behavior, 2010, 19, 467-473.	1.7	37
53	In vivo P-glycoprotein function before and after epilepsy surgery. Neurology, 2014, 83, 1326-1331.	1.1	37
54	Effects of norepinephrine transporter gene variants on <scp>NET</scp> binding in <scp>ADHD</scp> and healthy controls investigated by <scp>PET</scp> . Human Brain Mapping, 2016, 37, 884-895.	3.6	37

#	Article	IF	CITATIONS
55	In vivo and in vitro evaluation of [18 F]FETO with respect to the adrenocortical and GABAergic system in rats. European Journal of Nuclear Medicine and Molecular Imaging, 2003, 30, 1398-1401.	6.4	35
56	Task-relevant brain networks identified with simultaneous PET/MR imaging of metabolism and connectivity. Brain Structure and Function, 2018, 223, 1369-1378.	2.3	34
57	[18F]FETO for adrenocortical PET imaging: a pilot study in healthy volunteers. European Journal of Nuclear Medicine and Molecular Imaging, 2006, 33, 669-672.	6.4	33
58	Multimodal imaging of human early visual cortex by combining functional and molecular measurements with fMRI and PET. NeuroImage, 2008, 41, 204-211.	4.2	32
59	¹¹ C-Methionine PET/CT Imaging of ^{99m} Tc-MIBI-SPECT/CT-Negative Patients With Primary Hyperparathyroidism and Previous Neck Surgery. Journal of Clinical Endocrinology and Metabolism, 2014, 99, 4199-4205.	3.6	32
60	Association of Protein Distribution and Gene Expression Revealed by PET and Post-Mortem Quantification in the Serotonergic System of the Human Brain. Cerebral Cortex, 2017, 27, 117-130.	2.9	30
61	Prospective evaluation of the performance of [68Ga]Ga-PSMA-11 PET/CT(MRI) for lymph node staging in patients undergoing superextended salvage lymph node dissection after radical prostatectomy. European Journal of Nuclear Medicine and Molecular Imaging, 2019, 46, 2169-2177.	6.4	30
62	Simple and fully automated preparation of [carbonyl-11C]WAY-100635. Radiochimica Acta, 2007, 95, .	1.2	28
63	Preparation and first evaluation of [18F]FE@SUPPY: a new PET tracer for the adenosine A3 receptor. Nuclear Medicine and Biology, 2008, 35, 61-66.	0.6	28
64	[18F]FE@SNAP—A new PET tracer for the melanin concentrating hormone receptor 1 (MCHR1): Microfluidic and vessel-based approaches. Bioorganic and Medicinal Chemistry, 2012, 20, 5936-5940.	3.0	28
65	Cerebral serotonin transporter asymmetry in females, males and male-to-female transsexuals measured by PET in vivo. Brain Structure and Function, 2014, 219, 171-183.	2.3	28
66	Evaluation of fatty acid synthase in prostate cancer recurrence: SUV of [¹¹ C]acetate PET as a prognostic marker. Prostate, 2015, 75, 1760-1767.	2.3	28
67	Preparation and pre-vivo evaluation of no-carrier-added, carrier-added and cross-complexed [68Ca]-EDTMP formulations. European Journal of Pharmaceutics and Biopharmaceutics, 2008, 68, 406-412.	4.3	27
68	Simple and rapid preparation of [11C]DASB with high quality and reliability for routine applications. Applied Radiation and Isotopes, 2009, 67, 1654-1660.	1.5	27
69	Serotonin-1A receptor binding is positively associated with gray matter volume — A multimodal neuroimaging study combining PET and structural MRI. NeuroImage, 2012, 63, 1091-1098.	4.2	27
70	Optimization of the radiosynthesis of the Alzheimer tracer 2-(4-N-[11C]methylaminophenyl)-6-hydroxybenzothiazole ([11C]PIB). Applied Radiation and Isotopes, 2011, 69, 1212-1217.	1.5	26
71	An Overview of PET Radiochemistry, Part 1: The Covalent Labels ¹⁸ F, ¹¹ C, and ¹³ N. Journal of Nuclear Medicine, 2018, 59, 1350-1354.	5.0	26
72	Microfluidic preparation of [18F]FE@SUPPY and [18F]FE@SUPPY:2 — comparison with conventional radiosyntheses. Nuclear Medicine and Biology, 2011, 38, 427-434.	0.6	25

#	Article	IF	CITATIONS
73	Radiolabeling of [18F]altanserin — a microfluidic approach. Nuclear Medicine and Biology, 2012, 39, 1087-1092.	0.6	25
74	Impact of hybrid PET/MR technology on multiparametric imaging and treatment response assessment of cervix cancer. Radiotherapy and Oncology, 2017, 125, 420-425.	0.6	25
75	On the relationship of first-episode psychosis to the amphetamine-sensitized state: a dopamine D2/3 receptor agonist radioligand study. Translational Psychiatry, 2020, 10, 2.	4.8	25
76	New approaches for the reliable in vitro assessment of binding affinity based on high-resolution real-time data acquisition of radioligand-receptor binding kinetics. EJNMMI Research, 2017, 7, 22.	2.5	24
77	EGFR is required for FOSâ€dependent bone tumor development via RSK2/CREB signaling. EMBO Molecular Medicine, 2018, 10, .	6.9	24
78	The effect of electroconvulsive therapy on cerebral monoamine oxidase A expression in treatment-resistant depression investigated using positron emission tomography. Brain Stimulation, 2019, 12, 714-723.	1.6	24
79	Effects of hormone replacement therapy on cerebral serotonin-1A receptor binding in postmenopausal women examined with [carbonyl-11C]WAY-100635. Psychoneuroendocrinology, 2014, 45, 1-10.	2.7	23
80	Association of norepinephrine transporter methylation with in vivo NET expression and hyperactivity–impulsivity symptoms in ADHD measured with PET. Molecular Psychiatry, 2021, 26, 1009-1018.	7.9	23
81	Synthesis of [18F]FETO, a novel potential 11-? hydroxylase inhibitor. Journal of Labelled Compounds and Radiopharmaceuticals, 2003, 46, 379-388.	1.0	22
82	The influence of the rs6295 gene polymorphism on serotonin-1A receptor distribution investigated with PET in patients with major depression applying machine learning. Translational Psychiatry, 2017, 7, e1150-e1150.	4.8	22
83	Assessment of Ketamine Binding of the Serotonin Transporter in Humans with Positron Emission Tomography. International Journal of Neuropsychopharmacology, 2018, 21, 145-153.	2.1	22
84	Visual and semiquantitative 11C-methionine PET: an independent prognostic factor for survival of newly diagnosed and treatment-naÃ ⁻ ve gliomas. Neuro-Oncology, 2018, 20, 411-419.	1.2	22
85	Brain monoamine oxidase A in seasonal affective disorder and treatment with bright light therapy. Translational Psychiatry, 2018, 8, 198.	4.8	22
86	Altered interregional molecular associations of the serotonin transporter in attention deficit/hyperactivity disorder assessed with PET. Human Brain Mapping, 2017, 38, 792-802.	3.6	21
87	Utility of Absolute Quantification in Non-lesional Extratemporal Lobe Epilepsy Using FDG PET/MR Imaging. Frontiers in Neurology, 2020, 11, 54.	2.4	21
88	Prediction of response and survival after standardized treatment with 7400ÂMBq 177Lu-PSMA-617 every 4Âweeks in patients with metastatic castration-resistant prostate cancer. European Journal of Nuclear Medicine and Molecular Imaging, 2021, 48, 1650-1657.	6.4	21
89	Binding studies of [18F]-fluoride and polyphosphonates radiolabelled with [99mTc], [111In], [153Sm] and [188Re] on bone compartments: Verification of the pre vivo model?. Bone, 2005, 37, 404-412.	2.9	20
90	18F fluoroethylations: different strategies for the rapid translation of 11C-methylated radiotracers. Nuclear Medicine and Biology, 2007, 34, 1019-1028.	0.6	20

#	Article	IF	CITATIONS
91	Preclinical in vitro & in vivo evaluation of [11C]SNAP-7941 – the first PET tracer for the melanin concentrating hormone receptor 1. Nuclear Medicine and Biology, 2013, 40, 919-925.	0.6	20
92	Reliable set-up for in-loop 11C-carboxylations using Grignard reactions for the preparation of [carbonyl-11C]WAY-100635 and [11C]-(+)-PHNO. Applied Radiation and Isotopes, 2013, 82, 75-80.	1.5	20
93	The value of [11C]-acetate PET and [18F]-FDG PET in hepatocellular carcinoma before and after treatment with transarterial chemoembolization and bevacizumab. European Journal of Nuclear Medicine and Molecular Imaging, 2017, 44, 1732-1741.	6.4	20
94	A Microdosing Study with ^{99m} Tc-PHC-102 for the SPECT/CT Imaging of Primary and Metastatic Lesions in Renal Cell Carcinoma Patients. Journal of Nuclear Medicine, 2021, 62, 360-365.	5.0	20
95	New aspects on the preparation of [11C]acetate—a simple and fast approach via distillation. Applied Radiation and Isotopes, 2004, 61, 1147-1150.	1.5	19
96	[18F]FETO: metabolic considerations. European Journal of Nuclear Medicine and Molecular Imaging, 2006, 33, 928-931.	6.4	19
97	Combining image-derived and venous input functions enables quantification of serotonin-1A receptors with [carbonyl-11C]WAY-100635 independent of arterial sampling. NeuroImage, 2012, 62, 199-206.	4.2	19
98	Relation of progesterone and DHEAS serum levels to 5-HT1A receptor binding potential in pre- and postmenopausal women. Psychoneuroendocrinology, 2014, 46, 52-63.	2.7	19
99	Simple and rapid quantification of serotonin transporter binding using [11C]DASB bolus plus constant infusion. Neurolmage, 2017, 149, 23-32.	4.2	19
100	Progesterone Level Predicts Serotonin-1A Receptor Binding in the Male Human Brain. Neuroendocrinology, 2011, 94, 84-88.	2.5	18
101	Bone lesion detection with carrier-added 99mTc-EDTMP in comparison with 99mTc-DPD. Nuclear Medicine Communications, 2004, 25, 361-365.	1.1	17
102	[18F]FMeNER-D2: Reliable fully-automated synthesis for visualization of the norepinephrine transporter. Nuclear Medicine and Biology, 2013, 40, 1049-1054.	0.6	17
103	Hide and seek: a comparative autoradiographic in vitro investigation of the adenosine A3 receptor. European Journal of Nuclear Medicine and Molecular Imaging, 2015, 42, 928-939.	6.4	17
104	Development of a Novel Nonpeptidic ¹⁸ F-Labeled Radiotracer for in Vivo Imaging of Oxytocin Receptors with Positron Emission Tomography. Journal of Medicinal Chemistry, 2016, 59, 1800-1817.	6.4	17
105	Expanding LogP: Present possibilities. Nuclear Medicine and Biology, 2018, 58, 20-32.	0.6	17
106	Thyroid and androgen receptor signaling are antagonized by μ rystallin in prostate cancer. International Journal of Cancer, 2021, 148, 731-747.	5.1	17
107	Binding studies of [18F]-fluoride and polyphosphonates radiolabelled with [111In], [99mTc], [153Sm], and [188Re] on bone compartments: a new model for the pre vivo evaluation of bone seekers?. Bone, 2004, 34, 835-844.	2.9	16
108	Synthesis and biodistribution of [18F]FE@CIT, a new potential tracer for the dopamine transporter. Synapse, 2005, 55, 73-79.	1.2	16

MARKUS MITTERHAUSER

#	Article	IF	CITATIONS
109	Nebivolol treatment increases splanchnic blood flow and portal pressure in cirrhotic rats via modulation of nitric oxide signalling. Liver International, 2013, 33, 561-568.	3.9	16
110	Parameter evaluation and fully-automated radiosynthesis of [11 C]harmine for imaging of MAO-A for clinical trials. Applied Radiation and Isotopes, 2015, 97, 182-187.	1.5	16
111	Changes in Tumor Biology During Chemoradiation of Cervix Cancer Assessed by Multiparametric MRI and Hypoxia PET. Molecular Imaging and Biology, 2018, 20, 160-169.	2.6	16
112	Hypothalamic serotonin-1A receptor binding measured by PET predicts the plasma level of dehydroepiandrosterone sulfate in healthy women. Neuroscience Letters, 2010, 476, 161-165.	2.1	15
113	[18F]FE@SUPPY and [18F]FE@SUPPY:2 — metabolic considerations. Nuclear Medicine and Biology, 2010, 37, 421-426.	0.6	15
114	Radiosynthesis of [11C]SNAP-7941—the first PET-tracer for the melanin concentrating hormone receptor 1 (MCHR1). Applied Radiation and Isotopes, 2012, 70, 2287-2294.	1.5	15
115	[¹⁸ F]FEPPA: Improved Automated Radiosynthesis, Binding Affinity, and Preliminary in Vitro Evaluation in Colorectal Cancer. ACS Medicinal Chemistry Letters, 2018, 9, 177-181.	2.8	15
116	Detection of Bone Metastases Using 11C-Acetate PET in Patients with Prostate Cancer with Biochemical Recurrence. Anticancer Research, 2015, 35, 6787-91.	1.1	15
117	Optimization of [11C]DASB-synthesis: Vessel-based and flow-through microreactor methods. Applied Radiation and Isotopes, 2012, 70, 2615-2620.	1.5	14
118	Preparation and First Preclinical Evaluation of [18F]FE@SNAP: A Potential PET Tracer for the Melanin Concentrating Hormone Receptor 1 (MCHR1). Scientia Pharmaceutica, 2013, 81, 625-639.	2.0	14
119	(R)-[18F]NEBIFQUINIDE: A promising new PET tracer for TSPO imaging. European Journal of Medicinal Chemistry, 2019, 176, 410-418.	5.5	14
120	First-in-human brain PET imaging of the GluN2B-containing N-methyl-D-aspartate receptor with (R)-11C-Me-NB1. Journal of Nuclear Medicine, 2021, , jnumed.121.262427.	5.0	14
121	Imaging Biomarkers or Biomarker Imaging?. Pharmaceuticals, 2014, 7, 765-778.	3.8	13
122	Impact of COMT genotype on serotonin-1A receptor binding investigated with PET. Brain Structure and Function, 2014, 219, 2017-2028.	2.3	13
123	Binding Affinity of Some Endogenous and Synthetic TSPO Ligands Regarding the rs6971 Polymorphism. International Journal of Molecular Sciences, 2019, 20, 563.	4.1	13
124	Radiosynthesis of 3-(2′-[18F]fluoro)-flumazenil ([18F]FFMZ). Journal of Labelled Compounds and Radiopharmaceuticals, 2003, 46, 1229-1240.	1.0	12
125	Interaction between 5-HTTLPR and 5-HT1B genotype status enhances cerebral 5-HT1A receptor binding. NeuroImage, 2015, 111, 505-512.	4.2	12
126	Parcellation of the Human Cerebral Cortex Based on Molecular Targets in the Serotonin System Quantified by Positron Emission Tomography In vivo. Cerebral Cortex, 2019, 29, 372-382.	2.9	12

#	Article	IF	CITATIONS
127	Speed matters to raise molar radioactivity: Fast HPLC shortens the quality control of C-11 PET-tracers. Nuclear Medicine and Biology, 2018, 57, 28-33.	0.6	12
128	Metabolic and pharmacokinetic considerations in the design of 2-phenyl substituted metyrapone derivatives: 2-methoxyphenylmetyrapone as a radioligand for functional diagnosis of adrenal pathology. Nuclear Medicine and Biology, 1995, 22, 1067-1074.	0.6	11
129	Labelling of EDTMP (Multibone®) with [111In], [99mTc] and [188Re] using different carriers for "cross complexation― Applied Radiation and Isotopes, 2004, 60, 653-658.	1.5	11
130	Imaging of adrenocortical metastases with [11C]metomidate. European Journal of Nuclear Medicine and Molecular Imaging, 2006, 33, 974-974.	6.4	11
131	Development and automation of a novel NET-PET tracer: [11C]Me@APPI. Nuclear Medicine and Biology, 2013, 40, 295-303.	0.6	11
132	Radiosynthesis and first preclinical evaluation of the novel norepinephrine transporter pet-ligand [11C]ME@HAPTHI. EJNMMI Research, 2015, 5, 113.	2.5	11
133	In vivo magnetic resonance imaging of pancreatic tumors using iron oxide nanoworms targeted with PTR86 peptide. Colloids and Surfaces B: Biointerfaces, 2017, 158, 423-430.	5.0	11
134	Modeling the acute pharmacological response to selective serotonin reuptake inhibitors in human brain using simultaneous PET/MR imaging. European Neuropsychopharmacology, 2019, 29, 711-719.	0.7	11
135	Association of dopamine D2/3 receptor binding potential measured using PET and [11C]-(+)-PHNO with post-mortem DRD2/3 gene expression in the human brain. NeuroImage, 2020, 223, 117270.	4.2	11
136	PSMA Expression in 122 Treatment Naive Glioma Patients Related to Tumor Metabolism in 11C-Methionine PET and Survival. Journal of Personalized Medicine, 2021, 11, 624.	2.5	11
137	Exploring the Impact of BDNF Val66Met Genotype on Serotonin Transporter and Serotonin-1A Receptor Binding. PLoS ONE, 2014, 9, e106810.	2.5	11
138	A general method for the fluorine-18 labelling of fluoroquinolone antibiotics. Journal of Labelled Compounds and Radiopharmaceuticals, 2003, 46, 715-727.	1.0	10
139	Impact of electroconvulsive therapy on 5-HT1A receptor binding in major depression. Molecular Psychiatry, 2013, 18, 1-1.	7.9	10
140	Comparative autoradiographic in vitro investigation of melanin concentrating hormone receptor 1 ligands in the central nervous system. European Journal of Pharmacology, 2014, 735, 177-183.	3.5	10
141	Comparison of fully-automated radiosyntheses of [11C]erlotinib for preclinical and clinical use starting from in target produced [11C]CO2 or [11C]CH4. EJNMMI Radiopharmacy and Chemistry, 2018, 3, 8.	3.9	10
142	Topologically Guided Prioritization of Candidate Gene Transcripts Coexpressed with the 5-HT1A Receptor by Combining In Vivo PET and Allen Human Brain Atlas Data. Cerebral Cortex, 2020, 30, 3771-3780.	2.9	10
143	Identification of tumor tissue-derived DNA methylation biomarkers for the detection and therapy response evaluation of metastatic castration resistant prostate cancer in liquid biopsies. Molecular Cancer, 2022, 21, 7.	19.2	10
144	The labelling of Nanocoll® with [111In] for dual-isotope scanning. Applied Radiation and Isotopes, 2003, 59, 337-342.	1.5	9

#	Article	IF	CITATIONS
145	In vitro evaluation of no carrier added, carrier added and cross-complexed [90Y]-EDTMP provides evidence for a novel "foreign carrier theory― Nuclear Medicine and Biology, 2006, 33, 95-99.	0.6	9
146	Development of potential selective and reversible pyrazoline based MAO-B inhibitors as MAO-B PET tracer precursors and reference substances for the early detection of Alzheimer's disease. Bioorganic and Medicinal Chemistry Letters, 2014, 24, 4490-4495.	2.2	9
147	Microfluidic ⁶⁸ Ga-labeling: a proof of principle study. Dalton Transactions, 2018, 47, 5997-6004.	3.3	9
148	Comparison of three different purification methods for the routine preparation of [11C] Metomidate. Applied Radiation and Isotopes, 2003, 59, 125-128.	1.5	8
149	What to consider in the development of new bone seekers: mechanistic and tracer-related aspects. Nuclear Medicine and Biology, 2008, 35, 817-824.	0.6	8
150	Synthesis of in vivo Metabolites of the New Adenosine A3 Receptor PET-Radiotracer [18F]FE@SUPPY. Heterocycles, 2008, 75, 339.	0.7	8
151	Synthesis, radiosynthesis and first in vitro evaluation of novel PET-tracers for the dopamine transporter: [11C]IPCIT and [18F]FE@IPCIT. Bioorganic and Medicinal Chemistry, 2013, 21, 7562-7569.	3.0	8
152	[18F]FE@SNAP—a specific PET tracer for melanin-concentrating hormone receptor 1 imaging?. EJNMMI Research, 2016, 6, 31.	2.5	8
153	Development and evaluation of a rapid analysis for HEPES determination in 68Ga-radiotracers. EJNMMI Research, 2018, 8, 95.	2.5	8
154	Multimodal [18F]FDG PET/CT Is a Direct Readout for Inflammatory Bone Repair: A Longitudinal Study in TNFα Transgenic Mice. Journal of Bone and Mineral Research, 2019, 34, 1632-1645.	2.8	8
155	Enhanced arecoline derivatives as muscarinic acetylcholine receptor M1 ligands for potential application as PET radiotracers. European Journal of Medicinal Chemistry, 2020, 204, 112623.	5.5	8
156	Automatisation and First Evaluation of [18F]FE@SUPPY:2, an Alternative PET-Tracer for the Adenosine A3 Receptor: A Comparison with [18F]FE@SUPPY. The Open Nuclear Medicine Journal, 2009, 1, 15-23.	0.2	8
157	Radiosynthesis of the adenosine A3 receptor ligand 5-(2-[18F]fluoroethyl) 2,4-diethyl-3-(ethylsulfanylcarbonyl)- 6-phenylpyridine-5-carboxylate ([18F]FE@SUPPY). Radiochimica Acta, 2008, 96, .	1.2	7
158	Epistasis of HTR1A and BDNF risk genes alters cortical 5-HT1A receptor binding: PET results link genotype to molecular phenotype in depression. Translational Psychiatry, 2019, 9, 5.	4.8	7
159	Cross-Modality Imaging of Murine Tumor Vasculature—a Feasibility Study. Molecular Imaging and Biology, 2021, 23, 874-893.	2.6	7
160	Multiparametric [11C]Acetate positron emission tomography-magnetic resonance imaging in the assessment and staging of prostate cancer. PLoS ONE, 2017, 12, e0180790.	2.5	7
161	Development of a radiolabeled caninized anti-EGFR antibody for comparative oncology trials. Oncotarget, 2017, 8, 83128-83141.	1.8	7
162	The stability of methyl-, ethyl- and fluoroethylesters against carboxylesterases in vitro: there is no difference. Nuclear Medicine and Biology, 2011, 38, 13-17.	0.6	6

#	Article	IF	CITATIONS
163	Synthesis and in Silico Evaluation of Novel Compounds for PET-Based Investigations of the Norepinephrine Transporter. Molecules, 2015, 20, 1712-1730.	3.8	6
164	[18F]FMeNER-D2: A systematic in vitro analysis of radio-metabolism. Nuclear Medicine and Biology, 2016, 43, 490-495.	0.6	6
165	In vivo evaluation of radiotracers targeting the melanin-concentrating hormone receptor 1: [11C]SNAP-7941 and [18F]FE@SNAP reveal specific uptake in the ventricular system. Scientific Reports, 2017, 7, 8054.	3.3	6
166	Probing the association between serotonin-1A autoreceptor binding and amygdala reactivity in healthy volunteers. Neurolmage, 2018, 171, 1-5.	4.2	6
167	Serotonin Transporter Binding in the Human Brain After Pharmacological Challenge Measured Using PET and PET/MR. Frontiers in Molecular Neuroscience, 2019, 12, 172.	2.9	6
168	In vitro Radiopharmaceutical Evidence for MCHR1 Binding Sites in Murine Brown Adipocytes. Frontiers in Endocrinology, 2019, 10, 324.	3.5	6
169	Assessment of left and right ventricular functional parameters using dynamic dual-tracer [13N]NH3 and [18F]FDG PET/MRI. Journal of Nuclear Cardiology, 2022, 29, 1003-1017.	2.1	6
170	Response and Toxicity to the Second Course of 3 Cycles of 177Lu-PSMA Therapy Every 4 Weeks in Patients with Metastatic Castration-Resistant Prostate Cancer. Cancers, 2021, 13, 2489.	3.7	6
171	An in vitro model for the comparative evaluation of bone seeking pharmaceuticals. ALTEX: Alternatives To Animal Experimentation, 2008, 25, 51-55.	1.5	6
172	NCA nucleophilic radiofluorination on substituted benzaldehydes for the preparation of [18F]fluorinated aromatic amino acids. Applied Radiation and Isotopes, 2006, 64, 355-359.	1.5	5
173	Metabolism and autoradiographic evaluation of [18F]FE@CIT: a Comparison with [123I]β-CIT and [123I]FP-CIT. Nuclear Medicine and Biology, 2008, 35, 475-479.	0.6	5
174	Radiosynthesis of a novel potential adenosine A3 receptor ligand, 5-ethyl 2,4-diethyl-3-((2-[18F]fluoroethyl)sulfanylcarbonyl)-6-phenylpyridine-5-carboxylate ([18F]FE@SUPPY:2). Radiochimica Acta, 2009, 97, 753-758.	1.2	5
175	Syntheses of Precursors and Reference Compounds of the Melanin-Concentrating Hormone Receptor 1 (MCHR1) Tracers [11C]SNAP-7941 and [18F]FE@SNAP for Positron Emission Tomography. Molecules, 2013, 18, 12119-12143.	3.8	5
176	[18F]FE@SUPPY: a suitable PET tracer for the adenosine A3 receptor? An in vivo study in rodents. European Journal of Nuclear Medicine and Molecular Imaging, 2015, 42, 741-749.	6.4	5
177	A new method measuring the interaction of radiotracers with the human P-glycoprotein (P-gp) transporter. Nuclear Medicine and Biology, 2018, 60, 29-36.	0.6	5
178	Preclinical <i> In Vitro</i> and <i> In Vivo</i> Evaluation of [¹⁸ F]FE@SUPPY for Cancer PET Imaging: Limitations of a Xenograft Model for Colorectal Cancer. Contrast Media and Molecular Imaging, 2018, 2018, 1-9.	0.8	5
179	SNAPshots of the MCHR1: a Comparison Between the PET-Tracers [18F]FE@SNAP and [11C]SNAP-7941. Molecular Imaging and Biology, 2019, 21, 257-268.	2.6	5
180	Attenuation Correction Approaches for Serotonin Transporter Quantification With PET/MRI. Frontiers in Physiology, 2019, 10, 1422.	2.8	5

#	Article	IF	CITATIONS
181	Brain glucose uptake during transcranial direct current stimulation measured with functional [18F]FDG-PET. Brain Imaging and Behavior, 2020, 14, 477-484.	2.1	5
182	Disrupted relationship between blood glucose and brain dopamine D2/3 receptor binding in patients with first-episode schizophrenia. NeuroImage: Clinical, 2021, 32, 102813.	2.7	5
183	Inhibition of Lipid Accumulation in Skeletal Muscle and Liver Cells: A Protective Mechanism of Bilirubin Against Diabetes Mellitus Type 2. Frontiers in Pharmacology, 2020, 11, 636533.	3.5	5
184	Renal and Salivary Gland Functions after Three Cycles of PSMA-617 Therapy Every Four Weeks in Patients with Metastatic Castration-Resistant Prostate Cancer. Current Oncology, 2021, 28, 3692-3704.	2.2	5
185	Some new methods for the synthesis of cardiac neurotransmission PET radiotracers. Nuclear Medicine and Biology, 1995, 22, 1037-1043.	0.6	4
186	Molar activity – The keystone in 11C-radiochemistry: An explorative study using the gas phase method. Nuclear Medicine and Biology, 2018, 67, 21-26.	0.6	4
187	Sex-differences in [68Ga]Ga-DOTANOC biodistribution. Nuclear Medicine and Biology, 2019, 76-77, 15-20.	0.6	4
188	Advancing Biomarker Development Through Convergent Engagement: Summary Report of the 2nd International Danube Symposium on Biomarker Development, Molecular Imaging and Applied Diagnostics; March 14–16, 2018; Vienna, Austria. Molecular Imaging and Biology, 2020, 22, 47-65.	2.6	4
189	Single-lesion Prostate-specific Membrane Antigen Protein Expression (PSMA) and Response to [177Lu]-PSMA-ligand Therapy in Patients with Castration-resistant Prostate Cancer. European Urology Open Science, 2021, 30, 63-66.	0.4	4
190	Experimental Nuclear Medicine Meets Tumor Biology. Pharmaceuticals, 2022, 15, 227.	3.8	4
191	Urinary metabolic profile in rat of 1-(2-methoxyphenyl)-2-methyl-2-(3-pyridyl)-1-propanone: a potential radioligand for functional diagnosis of adrenal pathology. Xenobiotica, 1996, 26, 211-219.	1.1	3
192	Preparation and radiosynthesis of [18F]FE@CFN (2-[18F]fluoroethyl) Tj ETQq0 0 0 rgBT /Overlock 10 Tf 50 307 T receptor imaging agent. Radiochimica Acta, 2007, 95, .	d (4-[N-(1 1.2	-oxopropyl)-1 3
193	Quantification of the radio-metabolites of the serotonin-1A receptor radioligand [carbonyl-11C]WAY-100635 in human plasma: An HPLC-assay which enables measurement of two patients in parallel. Applied Radiation and Isotopes, 2012, 70, 2730-2736.	1.5	3
194	**-Postprandial pancreatic [11C]methionine uptake after pancreaticoduodenectomy mirrors basal beta cell function and insulin release. European Journal of Nuclear Medicine and Molecular Imaging, 2017, 44, 509-516.	6.4	3
195	Reconsider logP!. Nuclear Medicine and Biology, 2017, 54, 42.	0.6	3
196	[11C]acetate PET as a tool for diagnosis of liver steatosis. Abdominal Radiology, 2018, 43, 2963-2969.	2.1	3
197	L-[S-methyl-11C]methionine – An example of radiosynthetic optimization. Applied Radiation and Isotopes, 2018, 141, 107-111.	1.5	3
198	Synthesis and in vitro evaluation of new translocator protein ligands designed for positron emission tomography. Future Medicinal Chemistry, 2019, 11, 539-550.	2.3	3

#	Article	IF	CITATIONS
199	Characterization of Bone Lesions in Myeloma Before and During Anticancer Therapy Using ¹⁸ F-FDG-PET/CT and ¹⁸ F-NaF-PET/CT. Anticancer Research, 2019, 39, 1943-1952.	1.1	3
200	Synthesis of [68Ga]Gallium Dota-(Tyr3)-Octreotide Acetate ([68Ga]-Dotatoc). , 0, , 321-334.		3
201	Immune Checkpoint Inhibitor Therapy Induces Inflammatory Activity in the Large Arteries of Lymphoma Patients under 50 Years of Age. Biology, 2021, 10, 1206.	2.8	3
202	Clinical Value of 18F-fluorodihydroxyphenylalanine Positron Emission Tomography/Contrast-enhanced Computed Tomography (18F-DOPA PET/CT) in Patients with Suspected Paraganglioma. Anticancer Research, 2016, 36, 4187-93.	1.1	3
203	Cyclotrons Operated for Nuclear Medicine and Radiopharmacy in the German Speaking D-A-CH Countries: An Update on Current Status and Trends. Frontiers in Nuclear Medicine, 2022, 2, .	1.2	3
204	Spectral and chromatographic properties of 2-methoxyphenylmetyrapone and its potential metabolites. Journal of Pharmaceutical and Biomedical Analysis, 1997, 15, 479-486.	2.8	2
205	Radiopharmaceutical considerations on bone seeker uptake: should we learn from therapeutical targets of bisphosphonates?. Nuclear Medicine and Biology, 2011, 38, 617-618.	0.6	2
206	The Potential Role of the MCHR1 in Diagnostic Imaging: Facts and Trends. , 0, , .		2
207	Technical Aspect of the Automated Synthesis and Real-Time Kinetic Evaluation of [¹¹ C]SNAP-7941. Journal of Visualized Experiments, 2019, , .	0.3	2
208	Sorbitol as a Polar Pharmacological Modifier to Enhance the Hydrophilicity of 99mTc-Tricarbonyl-Based Radiopharmaceuticals. Molecules, 2020, 25, 2680.	3.8	2
209	If It Works, Don't Touch It? A Cell-Based Approach to Studying 2-[18F]FDG Metabolism. Pharmaceuticals, 2021, 14, 910.	3.8	2
210	Discovery of melaninâ€concentrating hormone receptor 1 in brown adipose tissue. Annals of the New York Academy of Sciences, 2021, 1494, 70-86.	3.8	2
211	Simultaneous analysis of 2-methoxyphenylmetyrapone and its seven potential metabolites by high-performance liquid chromatography. Biomedical Applications, 1997, 704, 315-323.	1.7	1
212	244 ANGIOGENESIS IN PORTAL HYPERTENSIVE NAD(P)HOXIDASE-KNOCKOUT-MICE IS MEDIATED BY A DIFFERENT PATHWAY THAN IN WILDTYPE ANIMALS. Journal of Hepatology, 2008, 48, S99.	3.7	1
213	Segmentation of [11C]DASB and [carbonyl-11C]WAY-100635 PET brain images using linear discriminant analysis. NeuroImage, 2010, 52, S155-S156.	4.2	1
214	PM478. Imaging the effects of d-amphetamine in the human brain for modelling dopaminergic alterations in schizophrenia. International Journal of Neuropsychopharmacology, 2016, 19, 74-74.	2.1	1
215	Attenuation of habenula–default mode network connectivity by selective serotonin reuptake inhibitors, a pharmacological hybrid PET/MR study. European Neuropsychopharmacology, 2016, 26, S317.	0.7	1
216	Monoamine oxidase A distribution volume as a correlate for electroconvulsive therapy – preliminary results. European Neuropsychopharmacology, 2017, 27, S708-S709.	0.7	1

MARKUS MITTERHAUSER

#	Article	IF	CITATIONS
217	Toward the Optimization of (+)-[11C]PHNO Synthesis: Time Reduction and Process Validation. Contrast Media and Molecular Imaging, 2019, 2019, 1-13.	0.8	1
218	Optimization of the Automated Synthesis of [11C]mHED—Administered and Apparent Molar Activities. Pharmaceuticals, 2019, 12, 12.	3.8	1
219	Feasibility and Optimal Time Point of [68Ga]Gallium-labeled Prostate-specific Membrane Antigen Ligand Positron Emission Tomography Imaging in Patients Undergoing Cytoreductive Surgery After Systemic Therapy for Primary Oligometastatic Prostate Cancer: Implications for Patient Selection and Extent of Surgery. European Urology Open Science. 2022. 40. 117-124.	0.4	1
220	Pharmacokinetics of 2-methoxyphenylmetyrapone and 2-bromophenylmetyrapone in rats. European Journal of Drug Metabolism and Pharmacokinetics, 1999, 24, 23-29.	1.6	0
221	Evaluation of novel tropane analogues. Nuclear Medicine and Biology, 2007, 34, 591-592.	0.6	0
222	S.07.04 Progesterone and estradiol plasma levels modulate serotonin-1A binding in the human brain. European Neuropsychopharmacology, 2008, 18, S168.	0.7	0
223	"Label and go―– A fast and easy radiolabelling method for pellets. Applied Radiation and Isotopes, 2010, 68, 399-403.	1.5	0
224	The "Drill & Fill" Method. Scientia Pharmaceutica, 2010, 78, 650-650.	2.0	0
225	FC10-05 - Attenuated serotonin transporter association between midbrain and nucleus accumbens in major depression. European Psychiatry, 2011, 26, 1868-1868.	0.2	0
226	Multimodal imaging of an astrocytoma affecting the amygdalar region. European Psychiatry, 2011, 26, 924-924.	0.2	0
227	Cortisol plasma levels are associated with serotonin - 1A receptor binding in postmenopausal women. European Psychiatry, 2011, 26, 933-933.	0.2	0
228	P.4.002 Serotonin transporter ratio between raphe nuclei and projection areas predicts SSRI treatment response in major depression. European Neuropsychopharmacology, 2012, 22, S85.	0.7	0
229	P.2.b.044 Serotonin transporter association between dorsal raphe and ventral striatum is diminished in major depression. European Neuropsychopharmacology, 2013, 23, S345.	0.7	0
230	A One-Step Microwave-Assisted Synthetic Method for an O/S-Chemoselective Route to Derivatives of the First Adenosine A3 PET Radiotracer. Molecules, 2014, 19, 4076-4082.	3.8	0
231	P.1.i.047 Interregional changes in serotonin transporter availability upon treatment with selective serotonin reuptake inhibitors. European Neuropsychopharmacology, 2015, 25, S327-S328.	0.7	0
232	2-Fluoro-N-methyl-N-({(3S,4S)-4-[2-(trifluoromethyl)phenoxy]-3,4-dihydro-1H-isochromen-3-yl}methyl)ethanamine MolBank, 2015, 2015, M858.	^{2.} 0.5	0
233	1-(3-Amino-1-phenylpropyl)-3-(2-fluorophenyl)-1,3-dihydro-2H-benzimidazol-2-one. MolBank, 2015, 2015, M867.	0.5	0
234	2-Fluoro-N-methyl-N-{[(3S*,4S*)-4-(2-methylphenoxy)-3,4-dihydro-1H-isochromen-3-yl]methyl}ethanamine. MolBank, 2015, 2015, M862.	0.5	0

#	Article	IF	CITATIONS
235	P.1.i.037 Effects of norepinephrine transporter gene variants on protein binding in patients with ADHD using PET. European Neuropsychopharmacology, 2015, 25, S321-S322.	0.7	ο
236	PS168. Hybrid PET/MR imaging of serotonin transporter occupancy and brain activation to elucidate the mechanism of action of selective serotonin reuptake inhibitors. International Journal of Neuropsychopharmacology, 2016, 19, 60-61.	2.1	0
237	Neurochemical and behavioral sensitization to d-amphetamine in healthy subjects measured with [¹¹ C]-(+)-PHNO-PET. European Psychiatry, 2016, 33, S105-S106.	0.2	Ο
238	Influence of serotonergic gene variants on serotonin transporter binding in ADHD. European Neuropsychopharmacology, 2017, 27, S707.	0.7	0
239	Investigating dose dependency of ketamine binding on the serotonin transporter with positron emission tomography. European Neuropsychopharmacology, 2017, 27, S779.	0.7	Ο
240	Characterization of pharmacological response to selective serotonin reuptake inhibitors using clustering of resting-state hybrid PET/MR data. European Neuropsychopharmacology, 2019, 29, S603-S604.	0.7	0
241	The relationship between cholecystokinin secretion and pancreatic [11C]methionine uptake in patients after partial pancreaticoduodenectomy. Annals of Nuclear Medicine, 2020, 34, 691-695.	2.2	Ο
242	Differential impact of radiation therapy after radical prostatectomy on recurrence patterns: an assessment using [68Ga]Ga-PSMA ligand PET/CT(MRI). Prostate Cancer and Prostatic Diseases, 2021, 24, 439-447.	3.9	0
243	Synthesis of 2-(4-N-[11C]Methylaminophenyl)-6-Hydroxybenzothiazole ([11C]6-OH-BTA-1; [11C]PIB). , 0, , 177-189.		Ο
244	Synthesis of 3-Amino-4-[2-(N-Methyl-N-[11C]Methyl-Amino-Methyl)Phenylsulfanyl]-Benzonitrile ([11C]DASB). , 0, , 285-296.		0
245	Explorative analysis of retrospective data of patients with esophageal cancer at the Department of Nuclear Medicine at the Medical University of Vienna: Predicting 30-month survival and progress-free survival using Supervised Machine Learning. Nuklearmedizin - NuclearMedicine, 2019, 58, .	0.7	0
246	Adrenal Carcinoma – Radionuclide Imaging. , 2009, , 29-42.		0
247	Simultaneous radiomethylation of [11C]harmine and [11C]DASB and kinetic modeling approach for serotonergic brain imaging in the same individual. Scientific Reports, 2022, 12, 3283.	3.3	Ο